Stoch Environ Res Risk Assess
DOI 10.1007/s00477-014-0887-2

ORIGINAL PAPER

Changing variance and skewness as leading indicators for detecting ozone exposure-associated lung function decrement

Nan-Hung Hsieh · Yi-Hsien Cheng · Chung-Min Liao

Abstract The objective of this study was to develop a novel risk analysis approach to assess ozone exposure as a risk factor for respiratory health. Based on the human exposure experiment, the study first constructed the relationship between lung function decrement and respiratory symptoms scores (ranged 0–1 corresponding to absent to severe symptoms). This study used a toxicodynamic model to estimate different levels of ozone exposure concentration-associated lung function decrement measured as percent forced expiratory volume in 1 s (%FEV_1). The relationships between 8-h ozone exposure and %FEV_1 decrement were also constructed with a concentration–response model. The recorded time series of environmental monitoring of ozone concentrations in Taiwan were used to analyze the statistical indicators which may have predictability in ozone-induced airway function disorders. A statistical indicator-based probabilistic risk assessment framework was used to predict and assess the ozone-associated respiratory symptoms scores. The results showed that ozone-associated lung function decrement can be detected by using information from statistical indicators. The coefficient of variation and skewness were the common indicators which were highly correlated with %FEV_1 decrement in the next 7 days. The model predictability can be further improved by a composite statistical indicator. There was a 50 % risk probability that mean and maximum respiratory symptoms scores would fall within the moderate region, 0.33–0.67, with estimates of 0.36 (95 % confidence interval 0.27–0.45) and 0.50 (0.41–0.59), respectively. We conclude that statistical indicators related to variability and skewness can provide a powerful tool for detecting ozone-induced health effects from empirical data in specific populations.

Keywords Ozone · Lung function · Statistical indicators · Toxicodynamic model · Time-series dynamics · Probabilistic risk assessment

1 Introduction

Ozone is among the most toxic oxidant air pollutants (Mudway and Kelly 2000). In the past decade, reported ozone-associated adverse health effects included airway inflammation and hyper-reactivity, exacerbations of bronchial asthma, and chronic obstructive pulmonary disease (COPD) (Mudway and Kelly 2000; Neuhaus-Steinmetz et al. 2000; McConnell et al. 2002; Backus et al. 2010). Certain individuals are particularly susceptible to this oxidant due to the fact that ozone may stimulate the release of endogenous mediators for airway inflammation. The inflammation further causes recurrent episodes of airflow obstruction-induced lung function changes. The vulnerable populations therefore experience the respiratory symptoms such as wheezing, breathlessness, chest tightness, and cough. Furthermore, biological plausibility for acute and chronic ozone effects on respiratory morbidity and mortality were evidenced by toxicological and human exposure studies, indicating that ozone affects airway inflammation, pulmonary function, asthma induction and exacerbation, and reduction of heart rate variability (Park et al. 2005; National Research Council 2008; Jerrett et al. 2009; Anenberg et al. 2010; Tank et al. 2011).

N.-H. Hsieh
Institute of Labor, Occupational Safety and Health, Ministry of Labor, New Taipei 22143, Taiwan, Republic of China

Y.-H. Cheng · C.-M. Liao (✉)
Department of Bioenvironmental Systems Engineering, National Taiwan University, Taipei 10617, Taiwan, Republic of China
e-mail: cmliao@ntu.edu.tw

Published online: 05 May 2014

Thus, an assessment of lung function decrement with regard to ozone exposure is essential for protection of the health of the public.

Mudway and Kelly (2000) indicated that even inhaling lightly elevated ozone concentrations could result in a range of respiratory symptoms including decreased lung function and increased airway hyper-reactivity in 10–20 % of the healthy population. McConnell et al. (2002) reported a significant increase in the incidence of new asthma diagnoses in association with heavy exercise in communities with high levels of ambient ozone. Jerrett et al. (2009) indicated that an increase in ozone concentration was highly likely to pose the risk of death from respiratory causes.

Ozone-associated lung inflammation can be characterized by polymorphonuclear leukocyte infiltration (Mudway and Kelly 2000). Ozone exposure also contributes to lung injury that may directly or indirectly affect adaptive immune responses such as T cell proliferation and response to allergen (Jakab et al. 1995; Inoue et al. 2000; Kleeberger et al. 2001; Depuydt et al. 2002; Fakhrzadeh et al. 2002; Tank et al. 2011). Lung diseases, such as asthma and COPD, have a tremendous impact on health and quality of life worldwide. For example, COPD, the fourth-leading cause of death in the United States, is the only major cause of death for which the age-adjusted death rate has increased in recent years (National Research Council 2008).

Despite the growing need to address the global impact of ozone-associated pulmonary diseases, it remains challenging to obtain the predictability of lung function decrement in a manner suitable for routine monitoring in humans. Dynamic modeling has played a key role in estimating ozone-associated lung function decrement (Freijer et al. 2002; McDonnell et al. 2010). These models all set out to assess the impact of different levels of ozone exposure on cellular damage-associated airway function effect induced by simulations with parameter values estimated from various data sources.

Recent studies addressing the risk of critical transitions in complex dynamic systems, ranging from medicine to climate and ecosystems, revealed that statistical indicators can be used as the early warning signals to capture predictability and detectability (Frey et al. 2005; Venegas et al. 2005 Carpenter and Brock 2006; Dakos et al. 2008; Guttal and Jayaprakash 2008; Biggs et al. 2009; Scheffer et al. 2009; Dakos et al. 2010; Drake and Griffen 2010). In an asthma study, Venegas et al. (2005) used the coefficient of variation as an indicator to assess the spatial heterogeneity of ventilation in the lung for understanding the lung function change during an acute asthma attack. Moreover, the coefficient of variation and skewness in lung function measurements have been used to assess the risk of future asthma episodes to improve the assessment and management of asthma severity (Frey et al. 2005). In the case of ecosystems, Drake and Griffen (2010) have shown that early warning signals of extinction risk in deteriorating environments can be detected by a composite indicator comprising the coefficient of variation, skewness, autocorrelation, and spatial correlation.

Taken together, these statistical indicators including the coefficient of variation (Frey et al. 2005; Carpenter and Brock 2006; Guttal and Jayaprakash 2008), skewness (Frey et al. 2005; Guttal and Jayaprakash 2008), autocorrelation (Dakos et al. 2008), and spatial correlation (Dakos et al. 2010, Drake and Griffen 2010) provide a powerful tool for detecting potential changes in systems from available measurements ranging from physiological and ecological systems to climate processes. Due to the nonlinear feature of ozone dynamics in the ambient environment, previous studies have used stochastic methods to predict ozone variations (Kim and Kumar 2005; Moral et al. 2014). However, those studies have not investigated whether the statistical properties embedded in ozone variation could be associated with lung function effects.

The purpose of this study was twofold: (1) to construct a dynamic model-based exposure–response profile describing the relationships between ozone exposure and lung function decrement from respiratory causes and (2) to develop a statistical indicator-based probabilistic risk assessment framework to detect and assess the ozone-associated lung function decrement. Our study provides a modeling approach that allows assessment of ozone-associated lung function decrement given that some information is available on the pulmonary ozone toxicity in susceptible individuals. From the prospects of health surveillance of chronic respiratory diseases, we hope that the proposed statistical indicator-based risk assessment scheme would enable the early identification of adverse health effects in specific populations.

2 Materials and methods

This study first collected and analyzed the human exposure experimental data. To estimate different levels of ozone exposure concentration-induced lung function decrement, the toxicodynamic model was refabricated. The concentration–response relationship between ozone exposure concentration and lung function decrement was further constructed by an empirical model. Moreover, the recorded time series of environmental ozone concentrations in Taiwan were transformed into statistical indicators to examine the predictability of ozone variability-associated airway function disorders. Finally, the statistical indicator-based probabilistic risk assessment framework was used to predict and assess the ozone exposure risk in percent forced expiratory volume in 1 s (%FEV_1) decrement.

2.1 Study data

To investigate the lung function decrement caused by ozone exposure, Schelegle et al. (2009) designed an inhalation experiment to observe the variations in FEV_1 during a 6.6-h ozone exposure. The valuable dataset obtained from the exposure experiment allowed us to examine the association between ozone exposure and health effects.

Briefly, 31 healthy adults (16 females and 15 males) aged 18–25 years were volunteered to challenge with the tolerable ozone in the stainless steel chamber. The exposure patterns included filtered air and four different ozone concentrations averaging 60, 70, 80, and 87 ppb. Each exposure pattern performed by each subject was conducted with a mean equivalent ventilation rate of 38.7 L min^{-1}. The recorded FEV_1 changing times were set on 1-, 2-, 3-, 4.6-, 5.6-, and 6.6-h post exposure, respectively, according to the original experimental design. During the study period, the subjects reported respiratory symptoms including throat tickle, cough, shortness of breath, and pain on deep inspiration. These symptoms were ranked based on the severity scale ranging from 0 to 40, representing absence to presence of severe respiratory symptoms. This study further normalized the score values to the range of 0–1 where ranges 0–0.33, 0.33–0.67, and 0.67–1 represent mild, moderate, and severe respiratory symptoms, respectively.

2.2 Time-series of ozone variability

The time-series dynamics of ozone data in Taiwan were adopted from the Taiwan Air Quality Monitoring Network for the period 2005–2009 (http://taqm.epa.gov.tw/taqm/en/default.aspx). We chose two traffic stations (Fushin and Fongshan) located at Kaohsiung City, the regions with the worst air quality in south Taiwan (Chen et al. 2003). The hourly monitoring data described clearly the distribution of ozone time-series dynamics. Compared with other cities, ozone concentrations in Kaohsiung City had higher frequency to exceed the air quality standard and was likely to harm the respiratory health of humans. The air quality guideline was assessed based on an 8-h peak daily exposure advised by World Health Organization (WHO) and U.S. Environmental Protection Agency (USEPA) (World Health Organization 2006; Weinhold 2008). Thus, we evaluated the exposure conditions by the daily readings generated from the 8-h peak ozone distributions.

2.3 Toxicodynamic modeling

A toxicologically based dynamic model developed by Freijer et al. (2002) was used to estimate ozone-associated lung function decrement and cellular injury/repair in lung surface. Here we used the toxicodynamic model (Freijer et al. 2002) incorporating the published human exposure data (Schelegle et al. 2009) to predict the ozone-associated exacerbations of lung function decrement. Thus our model is a direct generalization of the toxicodynamic model in Freijer et al. (2002).

We formulated the model as a system of ordinary differential equations as

$$\frac{dC_A}{dt} = p_A - (p_A + s_A + \dot{D})C_A, \tag{1}$$

$$\frac{dC_B}{dt} = p_B(1 - C_A(t - \tau)) - p_B C_B, \tag{2}$$

$$\frac{dF}{dt} = \alpha(1 - C_A - C_B)\dot{D} - k_F F, \tag{3}$$

where C_A and C_B are the cover ratio of the naive (type A) and oxidant-protective (type B) cells in the lung surface, respectively, F is the percent decrease in FEV_1 comparing with ozone non-exposure scenario, p_A and p_B are the natural turnover rate for naive and oxidants protective cells (h^{-1}), respectively, $\dot{D}$ is the ozone dose rate (mg h^{-1}), τ is the oxidants protective cells production delay time (h), α is the sensitization rate (mg^{-1}), and k_F is the desensitization rate (h^{-1}). The ozone dose rate ($\dot{D}$) can be obtained by multiplying ozone concentration (mg m^{-3}), inhalation rate (m^3 h^{-1}), and ozone reactive fraction of lung tissue (Gerrity and McDonnell 1989).

Due to the delay time in the production of type B cells, the present ozone exposure-based toxicodynamic model (Eq. 3) can be rewritten as follows under the short-term exposure scenario based on the human exposure experimental data,

$$\frac{dF}{dt} = \alpha(1 - C_A)\dot{D} - k_F F, \tag{4}$$

and the analytical solution of F is given by

$$F(t) = \frac{\alpha e^{-(\alpha+\beta)}(-1+\beta)(-e^{k_F t}k_F + e^{(k_F+\beta)t}k + e^{\beta t}\beta - e^{(k_F+\beta)t}\beta)}{\alpha\beta(\alpha-\beta)}, \tag{5}$$

where β is equal to $p_A + s_A\dot{D}$. Furthermore, the calculated ozone dose rates were set in different levels in the study period.

2.4 Statistical indicators

Drake and Griffen (2010) constructed a reliable research framework to predict and even forecast the ozone-associated exacerbations of lung function decrement. The principle of the research algorithm in this study was to integrate statistical indicators to improve predictability of the future events by historical time-series datasets. There are five

statistical indicators including standard deviation (SD), coefficient of variation (CV), skewness, coefficient of autocorrelation (CA), and coefficient of spatial correlation (CS).

The SD can be calculated as the sample standard deviation,

$$\mathrm{SD} = \sqrt{\frac{1}{n-1}\sum_{i=1}^{n}(x_i - \bar{x})^2}, \tag{6}$$

where n is sample size and $\bar{x}$ is sample mean. The CV can be calculated as the ratio of the sample standard deviation and sample mean as $\mathrm{CV} = \mathrm{SD}/\bar{x}$.

The sample skewness can be calculated by using the estimator g_1,

$$g_1 = \frac{m_3}{m_2^{3/2}}, \tag{7}$$

where m_2 is the sample variance SD^2 and m_3 is the sample third central moment as,

$$m_3 = \frac{1}{n}\sum_{i=1}^{n}(x_i - \bar{x})^3. \tag{8}$$

The CA corresponding to each sampling date can be calculated through the Pearson correlation coefficient (r) between the ozone concentrations at present and subsequent sampling times t and $t + \Delta t$ over all samples as,

$$r = \frac{\sum_{i=2}^{n}(x_i - \bar{x})(x_{i-1} - \bar{x})}{\sum_{i=1}^{n}(x_i - \bar{x})^2}. \tag{9}$$

Here we calculated the CA with 1 day lag. On the other hand, CS at each sampling date can be calculated by Spearman's rank correlation coefficient between two monitoring stations in the same time.

2.5 Composite standardized indices

Given absence of appropriate control group, a composite statistical indicator was used to provide an earlier and more accurate detection of the events (Drake and Griffen 2010). Since appropriate control groups are not typically available in the real world, Drake and Griffen (2010) introduced a method by rescaling each indicator on each sampling date by subtracting the running average from the start of the series and dividing by the running SD. Thus, this composite indicator (S) required no information about a control group and can be calculated as the sum of the standardized deviations of each statistical indicator from its long-run average.

Taking CV as an example, the standardized difference at time t can be written as

$$\hat{w}_t = \frac{w_t - \frac{1}{n}\sum_{k=1}^{t} w_k}{sd(w_\kappa)}, \tag{10}$$

where κ is the pooled time calculated over all sampling time ($\kappa \in 1,2,3, \ldots,t$) and $sd(w_\kappa)$ is the pooled SD in the progressive duration.

We then integrated these five distinct standardized indicators and determined the major related factors which can forecast the future ozone-associated events of lung function exacerbations as,

$$S = \hat{v}_t + \hat{w}_t + \hat{x}_t + \hat{y}_t + \hat{z}_t, \tag{11}$$

where $\hat{v}_t$, $\hat{w}_t$, $\hat{x}_t$, $\hat{y}_t$, and $\hat{z}_t$ represent the standardized SD, CV, CA, skewness, and CS, respectively. In this study, we calculated the monthly ozone monitoring data to forecast upcoming events. The composite indicator S can be used to predict the possible health effect in the next days. Here we used Pearson correlation analysis to determine the most correlated composite indicators.

2.6 Probabilistic risk model

We incorporated concentration–response analysis and statistical indicators to assess the risk for ozone-associated respiratory symptoms. To construct the concentration–response relationship, the 4-parameter nonlinear model was used to fit the study data (Hill 1910),

$$R(x) = R_{\min} + \frac{R_{\max} - R_{\min}}{1 + \left(\frac{\mathrm{E50}}{x}\right)^{n_{\mathrm{H}}}}, \tag{12}$$

where $R(x)$ is the lung function response caused by a specific ozone concentration x, $R_{\min}$ and $R_{\max}$, are the minimum and maximum responses, respectively, and E50 is the effective ozone concentration x causing 50 % of the maximum response, and n_{H} is the fitted Hill coefficient.

Risk characterization is the phase of risk assessment where the results of the ozone-associated lung function decrement and quantitative effect assessments are integrated to provide an estimate of risk. Applying the Hill-based dose–response model in Eq. (12), the cumulative distribution function (cdf) of the predicted normalized symptoms scores (SS) for a given $\%\mathrm{FEV}_1$ decrement can be expressed as the conditional cdf as $P(\mathrm{SS}|\mathrm{FEV}_1)$.

Thus, followed by the Bayesian inference, the exacerbations risk of respiratory symptoms (the posterior probability) can be calculated as the product of $P(\mathrm{FEV}_1)$ (the prior probability) and the conditional probability of $P(\mathrm{SS}|\mathrm{FEV}_1)$ (the likelihood). It results in a joint probability function or an exceedence profile, which describes the probability of exceeding particular symptoms scores associated with lung function decrement. This can be expressed mathematically as a probabilistic risk model,

$$P(R_{SS}) = P(FEV_1) \times P(SS|FEV_1), \quad (13)$$

where $P(R_{SS})$ represents the exacerbations risk of respiratory symptoms caused by ozone-associated lung function decrement and $P(FEV_1)$ is the probability density function of statistical indicators-based forecasted $\%FEV_1$ decrement in the specific stage. The exceedence risk profile can be obtained by $1 - P(R_{SS})$.

The probabilistic risk profiles can offer the reliable information to understand the expected risk. Each point on the risk curve represents both the probability that the respiratory system will be injured and also that the frequency with which that level of effect would be exceeded. Furthermore, the x-axis of the risk curve can be interpreted as a magnitude of effect (i.e., SS), and the y-axis can be interpreted as the probability that at least that magnitude of exacerbation effect will occur.

2.7 Uncertainty and data analysis

Uncertainty is a key component in risk assessment. In order to quantify the uncertainty and its impact on the estimation of expected risk, a Monte Carlo (MC) technique that can simulate the distribution of fitted parameters was implemented. A MC simulation was performed with 10,000 iterations to generate 2.5- and 97.5-percentiles as the 95 % confidence interval (CI) for all fitted models. The MC simulation was performed by using the Crystal Ball® software (Version 2000.2, Decisionerring, Inc., Denver, CO, USA). Optimal statistical models were selected on the basis of least squares criterion from a set of generalized linear and nonlinear models provided by TableCurve 2D packages (AISN Software Inc., Mapleton, OR, USA). The correlation analyses were performed by using Statisitca (Version 6.0, Statsoft Inc., Tulsa, OK, USA). The Berkeley Madonna (Version 8.3.9, Berkeley Madonna Inc., Berkeley, CA, USA) was employed to simulate the toxicodynamic model.

3 Results

3.1 Ozone-associated lung function decrement

Figure 1a, b shows the dynamics of concentration-specific symptoms scores and $\%FEV_1$ decrement varied with ozone levels ranging from 60 to 87 ppb. Here the time-course of symptoms scores (Fig. 1a) and $\%FEV_1$ decrement (Fig. 1b) in the ozone exposure experiment were coupled to construct a concentration–response profile describing the relationships between normalized symptoms scores and $\%FEV_1$ decrement (Fig. 1c). We found that the Hill model can well describe the relationship between $\%FEV_1$

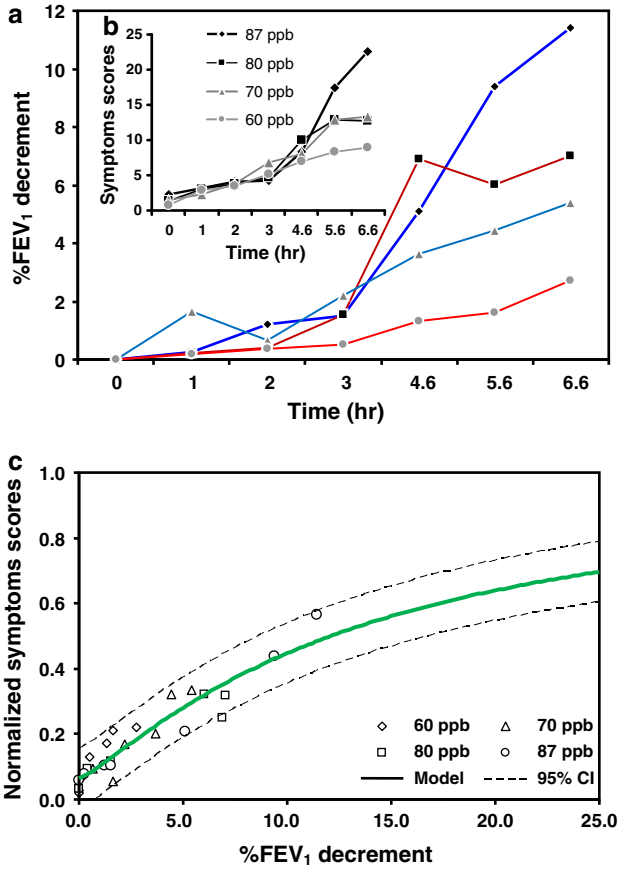

Fig. 1 Time course of **a** $\%FEV_1$ decrement and **b** symptoms scores under concentration-specific ozone exposures. **c** Reconstructed conditional probability fitted by a four parameter Hill model with 95 % confidence intervals describing the relationships between $\%FEV_1$ decrement and normalized symptoms scores

decrement and symptoms scores ($n_H = 1.2$, $r^2 = 0.89$, $p < 0.001$) in that the maximum symptoms scores can reach 0.99 with an effective $\%FEV_1$ decrement of 13.44 % (95 % CI 10.2–16.7) that causes 50 % maximum response (Fig. 1c).

To estimate the exacerbations risk of lung function during 8-h ozone exposure, the concentration-specific time-course of $\%FEV_1$ decrement data based on Schelegle et al. (2009) were used to simulate the progression of lung function changes (Fig. 2a–d). Table 1 summarizes the estimated model parameter values used for predicting ozone-associated lung function decrement and cellular injury. Our results showed that the fitted dynamic models could well illustrate the adverse FEV_1 progression during 8-h exposure (Fig. 2a–d). Figure 2a–d demonstrates that after 8-h exposure, FEV_1 decreased 5.7, 7.3, 9.0, and 10.2 % under ozone exposure doses of 60, 70, 80, and 87 ppb, respectively. Figure 2e shows an apparent agreement correlation between all the observed and predicted $\%FEV_1$ decrements in the whole calibration group ($r^2 = 0.73$).

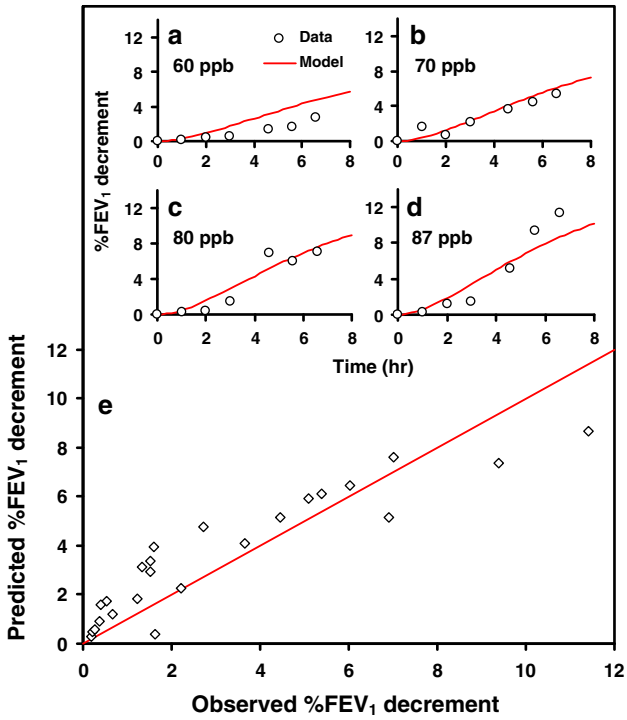

Fig. 2 Dynamic model predicted $\%FEV_1$ decrement dynamic under ozone exposure for (*a*, *b*) 60 ppb, (*c*, *d*) 70 ppb, (*e*, *f*) 80 ppb, and (*g*, *h*) 87 ppb, respectively

Table 1 Initial conditions and model parameter values used in this study

Symbol	Meaning	Unit	Value
Variable			
$C_A(0)$	Initial contribution proportion of type A cell		1
$C_B(0)$	Initial contribution proportion of type B cell		0
$F(0)$	$\%FEV_1$ decrement before exposure		0
$\dot{D}$	Ozone dose rate	mg h^{-1}	Varied[a]
Parameter			
p_A	Nature turnover rate for type A cell	h^{-1}	3×10^{-3}[b]
s_A	Oxidative decay constant	mg^{-1}	0.6[c]
p_B	Nature turnover rate for type B cell	h^{-1}	0.038[b]
α	Sensitization rate	mg^{-1}	18[c]
k_F	Desensitization rate	h^{-1}	0.42[c]
τ	Delay time of type B cell production	h	24[b]

[a] Ozone dose rates were estimated to be 0.247, 0.287, 0.329, and 0.358 mg for exposure ozone concentrations of 60, 70, 80, and 87 ppb, respectively

[b] Adopted from Freijer et al. (2002)

[c] Fitted from human experiment data

Given the estimated $\%FEV_1$ decrement for 8-h ozone exposure, the concentration–response relationships of continuous ozone exposure and $\%FEV_1$ decrement during the 8-h exposure can be constructed (Fig. 3). Our result indicated that the Hill model adequately fitted with the data ($r^2 = 0.99$, $p < 0.001$). The fitted parameters revealed that the maximum $\%FEV_1$ decrement can reach to 32.6 %. The EC50 estimate was 129.7 ppb (95 % CI 115.9–143.8). The fitted n_H was 2, indicating that the ozone exposure dose can significantly cause acute lung function exacerbations.

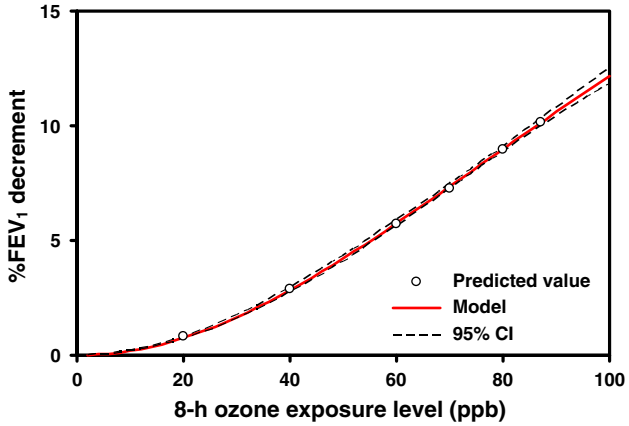

Fig. 3 Reconstructed Hill model-based concentration-response profiles for continuous 8-h ozone-associated $\%FEV_1$ decrement

3.2 Dynamics of statistical indicators

Based on the fitted $\%FEV_1$ decrement-daily 8-h ozone exposure relations (Fig. 3), the time-series of daily 8-h mean ozone concentration in Fusing and Fongshan (Fig. 4a, c) can then be converted into $\%FEV_1$ decrement time-series dynamics in the period 2005–2009 (Fig. 4b, d). We found that the time-series of observed 8-h mean ozone concentrations ranged from 2.7 to 121.7 ppb at two study stations (Fig. 4a, c).

To compose the indicators, we first calculated five statistical indicators that have potential predictability to indicate the embedded trends and properties in ozone time-series dynamics (Fig. 4e–i). Results showed that five indicators all present non-stationary processes during observed periods. The CV of ozone time-series data ranged from 0.20 to 0.83, indicating high dispersion among each dataset (Fig. 4f). Similarly, high dispersion was also found in CA over time ranging from −0.22 to 0.87 (Fig. 4g). The results also showed that skewness experienced seasonality with an extreme value occurring in summer (Fig. 4h). On the other hand, CS had an average of 0.88, revealing high correlation between two stations (Fig. 4i).

After calculating the statistical indicators, we standardized the statistical indicators to investigate the correlations among each other (Table 2). The results showed that standardized CV ($\hat{w}_t$) had a relatively high correlation with

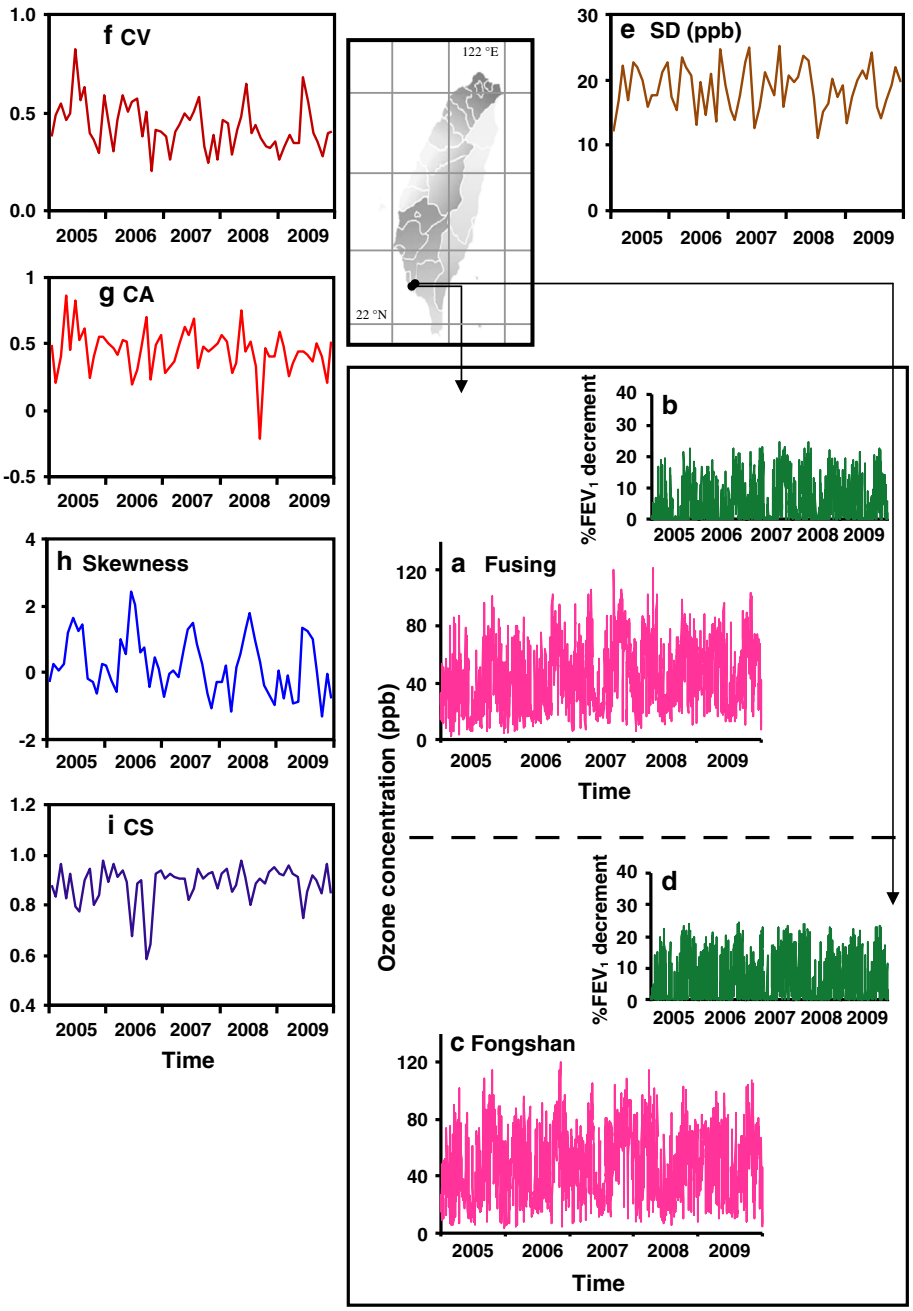

Fig. 4 Time series of daily 8-h ozone data with predicted ozone induced %FEV_1 decrement of **a**, **b** fusing and **c**, **d** Fongshan monitoring station in Kaohsiung for the period 2005–2009. The dynamics of statistical indicators including **e** standard deviation (SD), **f** coefficient of variation (CV), **g** coefficient of autocorrelation (CA), **h** skewness, and **i** coefficient of spatial correlation (CS) are calculated from monthly ozone recorded data

skewness ($\hat{y}_t$) ($r = 0.687$, $p < 0.0001$). To examine the forecasting capability for standardized indicators, we used a dynamics-based predictive model to transform the daily 8-h maximum ozone concentration to %FEV_1 decrement. We also found that $\hat{w}_t$ had better correlation with the next 7-day mean %FEV_1 decrements ($r = -0.515$, $p < 0.0001$) (Table 2). Thus, based on Pearson correlation analysis, the mean %FEV_1 decrements in the next 7 days can be assessed by one composite indicator $S_1 = \hat{w}_t + \hat{y}_t$, whereas the other one composite indicator $S_2 = \hat{w}_t + \hat{x}_t + \hat{y}_t + \hat{z}_t$ can be used to detect the maximum %FEV_1 decrements in the next 7 days (Table 2).

3.3 Composite indicator-based risk estimates

Our results showed that mean and maximum %FEV_1 decrement in the next 7 days had an apparent good association with the composite indicators of S_1 ($r = -0.571$, $p < 0.001$) and S_2 ($r = -0.554$, $p < 0.001$), respectively (Figs. 5a, 6a). These support the concept of using the

Table 2 Relative contributions of standardized statistical indicators to lung function decrement based on Pearson correlation coefficient (r)

	$\hat{v}_t$	$\hat{w}_t$	$\hat{x}_t$	$\hat{y}_t$	$\hat{z}_t$	F^{a}_{mean}	F^{b}_{MAX}
$\hat{v}_t$	1.000	0.324*	0.129	−0.253	0.266	0.067	−0.106
$\hat{w}_t$		1.000	0.205	0.687***	−0.107	−0.515***	−0.511***
$\hat{x}_t$			1.000	0.718	−0.150	−0.294	−0.233
$\hat{y}_t$				1.000	−0.341*	−0.532***	−0.358*
$\hat{z}_t$					1.000	0.0478	−0.130
F_{mean}						1.000	0.811***
F_{MAX}							1.000

Symbol meanings: $\hat{v}_t$: std standard deviation; $\hat{w}_t$: std coefficient of variation; $\hat{x}_t$: std coefficient of autocorrelation; $\hat{y}_t$: std skewness; $\hat{z}_t$: std spatial correlation

* $p < 0.05$, ** $p < 0.01$, *** $p < 0.0001$

[a] Mean %FEV_1 decrement in the next 7 days (%)

[b] Maximum %FEV_1 decrement in the next 7 days (%)

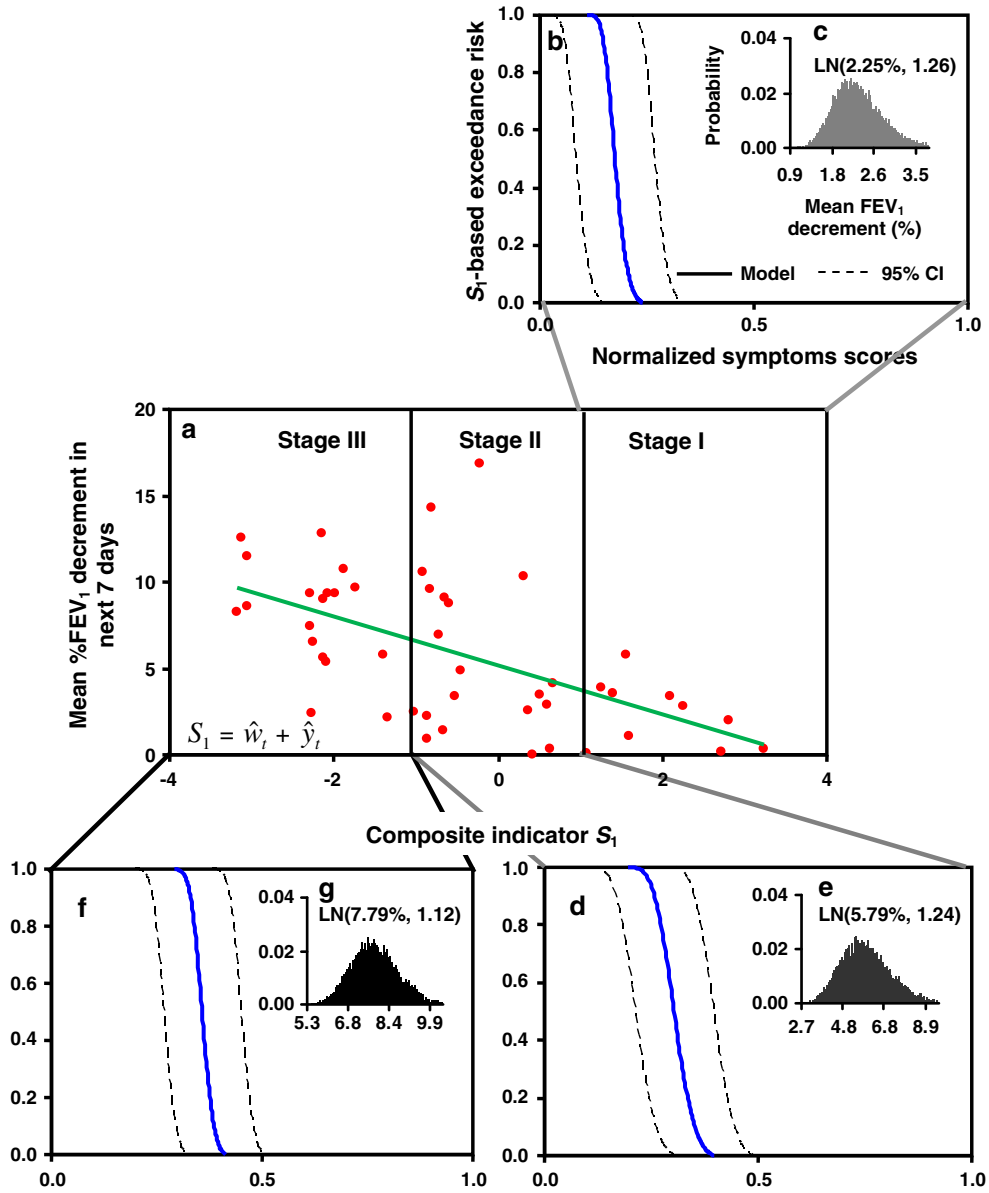

Fig. 5 **a** Linear regression analysis for forecasting mean %FEV_1 decrement based on the composite indicator S_1. The exceedance risk of normalized symptoms scores in stages of **b** I, **d** II, and **f** III based on representative probability density function of mean %FEV_1 decrement shown in **c**, **e**, and **g**, respectively

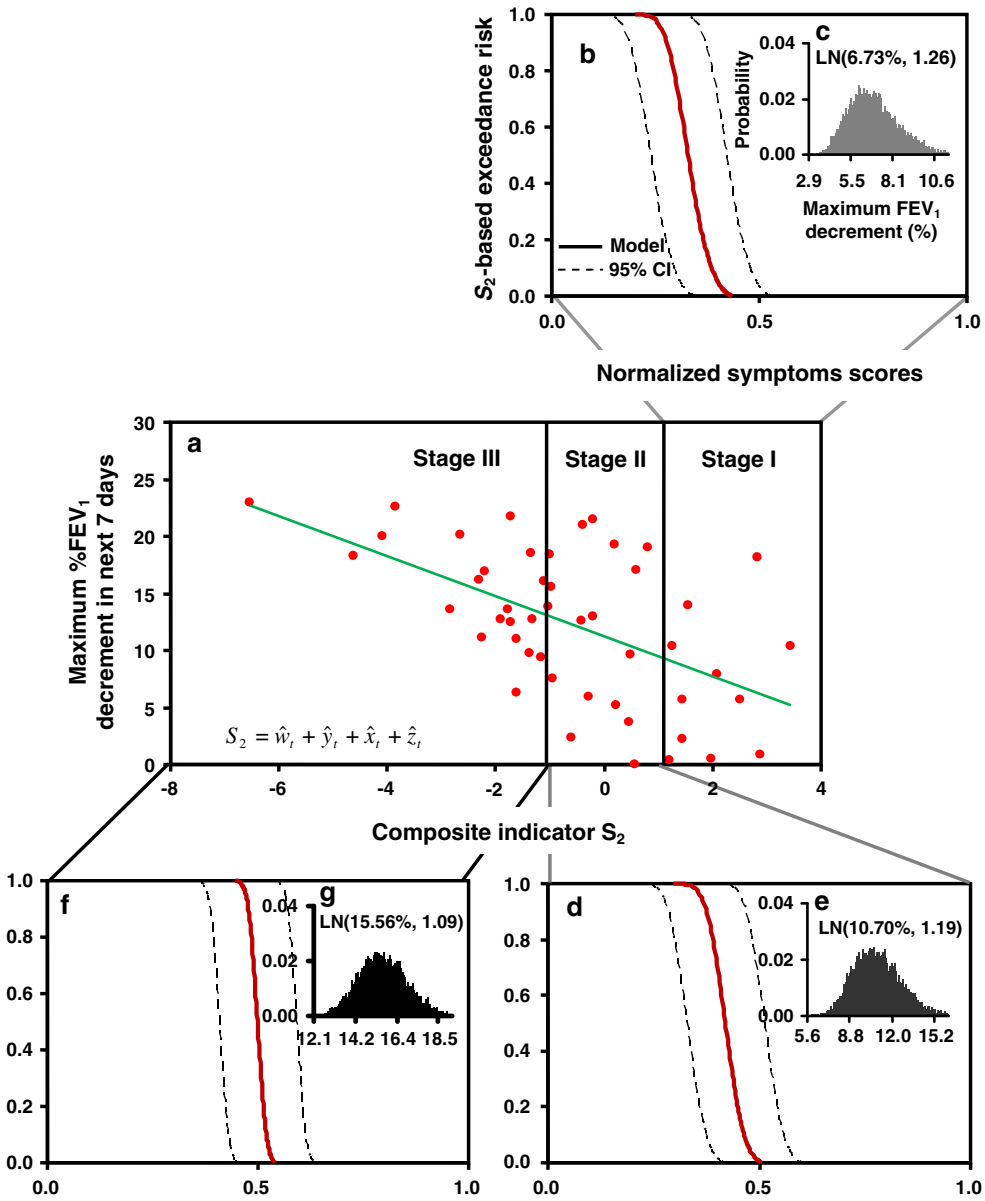

Fig. 6 **a** Linear regression analysis for forecasting maximum $\%FEV_1$ decrement based on the composite indicator S_2. The exceedance risk of normalized symptoms scores in stages of **b** I, **d** II, and **f** III based on representative probability density function of max $\%FEV_1$ decrement shown in **c**, **e**, and **g**, respectively

composite indictors as a proxy in the future events of $\%FEV_1$ decrement. Thus, S_1- and S_2-based risk estimates can then be calculated by the proposed probabilistic risk model (Eq. 13), respectively. Here we delineated ozone-associated respiratory symptoms elevation into three stages based on composite indicators in the range of -1 to 1. Thus, the calculated data for ozone concentration-based composite indicator can be rated uniformly (Figs. 5a, 6a).

Given the stage-specific FEV_1 pdf (Figs. 5c, g, e, 6c, g, e) and constructed concentration–response profile (Fig. 1c), the normalized symptoms scores at certain exceedance risk can be estimated based on composite indicators of S_1 and S_2, respectively (Figs. 5b, d, f, 6b, d, f; Table 3). Table 3 indicates that there was a 50 % probability for the mean symptoms scores exceeding 0.17 (95 % CI 0.08–0.27), 0.30 (0.21–0.39), and 0.36 (0.27–0.45) at stages I, II, and III, respectively. On the other hand, it is most likely that (80 % probability) the maximum symptoms scores will exceed 0.29 (0.20–0.39), 0.39 (0.30–0.48), and 0.48 (0.39–0.58), respectively, at stages I, II, and III (Table 3).

4 Discussion

4.1 Toxicodynamic modeling

In this study, we have developed a novel risk analysis approach which incorporated statistical indicators and probabilistic risk assessment to detect and assess the impact of ozone exposure on respiratory lung function

Table 3 Estimated mean and maximum normalized symptoms scores at exceedance risks 0.2, 0.5, and 0.8 based on composite indicators of S_1 and S_2, respectively, for ozone-associated respiratory symptoms elevation stages I (mild), II (moderate), and III (severe)

Symptoms		Exceedance risk	
Stage	0.8	0.5	0.2
Composite indicator S_1			
I	0.16 (0.07–0.25)[a]	0.17 (0.08–0.27)	0.20 (0.10–0.29)
II	0.27 (0.18–0.36)	0.30 (0.21–0.39)	0.34 (0.24–0.43)
III	0.34 (0.25–0.43)	0.36 (0.27–0.45)	0.38 (0.28–0.47)
Composite indicator S_2			
I	0.29 (0.20–0.39)	0.33 (0.24–0.42)	0.37 (0.27–0.46)
II	0.39 (0.30–0.48)	0.42 (0.33–0.51)	0.45 (0.36–0.54)
III	0.48 (0.39–0.58)	0.50 (0.41–0.59)	0.51 (0.42–0.61)

[a] Median (95 % CI)

decrement. Here, we used a Hill model to construct the relationship among lung function, respiratory symptoms and continuous ozone exposure because it is the biologically based concentration–response model (Goutelle et al. 2008). We showed that the Hill-based dose–response model can well describe the relationships between $\%FEV_1$ decrement and respiratory symptoms under the continuous ozone exposure.

On the other hand, we adopted a toxicodynamic model to predict ozone induced $\%FEV_1$ decrement under different exposure concentrations (Freijer et al. 2002). Freijer et al. (2002) considered the cell coverage mechanisms on the epithelium repair process of lung. However, in the model prediction of lung function changes, the adopted human experimental data was only performed in 6.6 h. We therefore assumed that the $\%FEV_1$ decrement between each date can be seen as a dependent process because it is difficult, if not impossible, to simulate ozone effects in the long-term exposure. Based on Freijer et al. (2002), the type B cells will be reactivated after the delay time of 24 h. Therefore, this study ignored the type B cell in the dynamic model. Furthermore, the model parameters in the toxicodynamic model capture the biological characteristics for epithelial cells and the physiological characteristics for lung function. To distinguish the different levels of ozone exposure that can cause lung function exacerbations, Freijer et al. (2002) suggested using lung function sensitization rate (α) and desensitization rate (k_F) which can be deduced from human exposure experiments.

However, there are some limitations in the toxicodynamic model incorporating with human exposure experiment. First, this study had only 4 exposure experimental datasets to generate the model prediction (Schelegle et al. 2009). The limited datasets may cause some errors in model predictions. Nevertheless, this study confirmed that the lung function decrement effects below 60 ppb can be well predicted by toxicodynamic and Hill model due to adequate fitting to human exposure experimental data. Second, the human experiment precisely defined patterns of exposure protocol, such as health status and exercise levels of participants. This well-controlled setting may have limits attempting to correspond to the real-world conditions. Third, the predictive values of lung function changes after continuous ozone exposure were simulated and extrapolated by the toxicodynamic model. Thus, the modeling approach laid out here may be extended in various directions. Moreover, other types of population heterogeneity can be taken into account, such as age-dependency and specific at-risk groups. Nevertheless, this study only focused on the daily maximum 8-h O_3 concentrations corresponding to the regulation for public health in time-series data analysis. Besides, the events of continuously high ozone concentration exposure-induced $\%FEV_1$ decrements in a day were not considered in this study.

4.2 Statistical indicators-based risk model

Our study found that standardized statistical indicators of CV and skewness had better correlations with mean $\%FEV_1$ decrement in the next 7 days. These results were also consistent with the asthma studies of Venegas et al. (2005) and Frey et al. (2005). Venegas et al. (2005) used CV as an indicator to capture the magnitude of change in a self-organized pattern of bronchoconstriction in human lungs in order to detect dangerous respiratory failure. Frey et al. (2005) used CV and skewness to assess the risk of lung function severity in asthmatics. In our study, no significant correlations were found among lung function decrement and statistical indicators of SD, CA, and CS. The results also revealed that there were weak correlations between lung function exacerbations and individual indicators. Thus, we incorporated standardized indicators of CA and CS into S_1 as a new composite S_2 for detecting the maximum $\%FEV_1$ decrement to further improve the predictability and detectability of lung function exacerbations.

Generally, the ozone concentrations are usually detected in low levels in ambient air. Based on the correlation analysis, the results found that high variability of ambient ozone had potential ability to give warning on the occurrence of high-level ozone in the next days. The increasingly positive skew of ozone concentration had similar function as variability that can reflect the increase in ozone-associated lung function decrement effect. Therefore, there are negative relationships between composite indicators and $\%FEV_1$ decrement. If the ambient ozone concentrations appeared highly variable in the past 1 month, it may implicate that the ozone-associated $\%FEV_1$ decrement will increase in the next 7 days.

Similarly, the increasing positive skew of ozone concentration can also reflect the increasing ozone-associated respiratory effects in the days after. The composite indicators had the best predictability for $\%FEV_1$ decrement in the next 7 days in our analysis. However, the correlation shows a decreasing trend when we consider a longer predicted period.

We also found that the probability of symptoms scores may fall into the worst stage if the composite indicators were less than -1, indicating that there was a 50 % risk probability for mean and maximum symptoms scores exceeding 0.38 and 0.50, respectively. McDonnell et al. (2010) have built an exposure–response model and proved that ozone may cause different levels of effect in the lifetime exposure. Therefore, it may be important to identify the age-specific adverse health effects by the toxicodynamic model-based risk assessment scheme in the future studies.

4.3 Implications

This study implicated that ozone exposure is a major risk factor for causing respiratory symptoms and lung function decrement. In addition, lung function is the robust marker to assess the adverse health effects posed by air pollution among general populations. We suggested that the risk of ozone-associated lung function decrement can be revealed by generic statistical indicators. The statistical indicators can give early warning on the possible respiratory effects caused by air pollution in the future. The new insight of this study concept can be used to improve the risk prediction in public health.

Recent studies indicated that traffic-related air pollution caused the onset of chronic pulmonary diseases in susceptible populations and even induced more severe respiratory illnesses (Chen et al. 2008; Balmes 2009). Currently, most epidemiological studies used statistical analyses such as the auto-regressive integrated moving average (ARIMA) to correlate environmental triggers and lung function-related diseases (Chen et al. 2006). In our case, for example, if we focused on a particular region with heavy air pollutions, we could scan data on time-series dynamics and spatial patterns of statistical indicators to detect which air pollutants may be a critical trigger in causing abnormal lung function. Subsequently, certain control measures could be targeted specifically at those major air pollutants.

The proposed probabilistic risk assessment framework could also link to a multidimensional approach including a combination of several clinical and physiological parameters such as symptoms, behavioral factors, lung function, and inflammatory markers which would be useful for detecting the future burden of respiratory-related illness that would result from air pollutants (Park et al. 2005; Anenberg et al. 2010; Tank et al. 2011). Therefore, statistical indicators are potentially powerful tools for assisting the scenario planning and forecasting those of increasing importance to environmental management and policy's decision-making.

This study found that composite statistical indicators can improve the predictability and detectability for ozone induced lung function decrement and respiratory symptoms. Our results revealed that the toxicodynamic model incorporating the statistical indicators-based risk assessment approach can be applied to human health exposure risk in the future. We hope that the proposed probabilistic risk assessment scheme can be used to (*i*) forecast the possible hazard under ozone exposure, (*ii*) reveal epidemiological phenomena caused by environmental stimuli, (*iii*) provide a novel method in risk assessment, and (*iv*) improve the risk estimates of lung function diseases as researches on chronic ozone exposure and illness continue growing globally. The study result also corresponded with our previous study which found that statistical indicators in fluctuating air pollution can be used to warn the risk of respiratory disease (Hsieh and Liao 2013).

The main conclusion from the work presented here is that ozone-associated lung function decrement can be assessed and detected by the information obtained from specific statistical indicators of critical lung function decreasing after the onset of environmental ozone exposure measured as daily 8-h exposure. Most importantly, we conclude that statistical indicators related to variability or skewness provide a powerful tool for empirical studies of environmental epidemiology or other complex systems (Scheffer et al. 2009; Drake and Griffen 2010). However, the perspective of identifying statistical indicators and exploring the possibilities and limitations of this emerging field are challenging, as the approach may provide an independent way to assess the risk of abnormal dynamic patterns of diseases in specific populations.

Acknowledgments The authors acknowledge the financial support of the National Science Council of Republic of China under Grant NSC 100-2313-B-002-012-MY3.

References

Anenberg SC, Horowitz LW, Tong DQ, West JJ (2010) An estimate of the global burden of anthropogenic ozone and fine particulate matter on premature human mortality using atmospheric modeling. Environ Health Perspect 118:1189–1195

Backus GS, Howden R, Fostel J, Bauer AK, Cho HY, Marzec J, Peden DB, Kleeberger SR (2010) Protective role of interleukin-10 in ozone-induced pulmonary inflammation. Environ Health Perspect 118:1721–1727

Balmes JR (2009) Can traffic-related air pollution cause asthma? Thorax 64:646–647

Biggs R, Carpenter SR, Brock WA (2009) Turning back from the brink: detecting an impending regime shift in time to avert it. Proc Natl Acad Sci USA 106:826–831

Carpenter SR, Brock WA (2006) Rising variance: a leading indicator of ecological transition. Ecol Lett 9:308–315

Chen KS, Ho YT, Chou YM (2003) Photochemical modeling and analysis of meteorological parameters during ozone episodes in Kaohsiung. Taiwan Atmos Environ 37:1811–1823

Chen CH, Xirasagar S, Lin HC (2006) Seasonality in adult asthma admissions, air pollutant levels, and climate: a population-based study. J Asthma 43:287–292

Chen E, Schreier HMC, Strunk RC, Brauer M (2008) Chronic traffic-related air pollution and stress interaction to predict biologic and clinical outcomes in asthma. Environ Health Perspect 116:970–975

Dakos V, Scheffer M, van Nes EH, Brovkin V, Petoukhov V, Held H (2008) Slowing down as an early warning signal for abrupt climate change. Proc Natl Acad Sci USA 105:14308–14312

Dakos V, van Nes EH, Donangelo R, Fort H, Scheffer M (2010) Spatial correlation as leading indicator of catastrophic shifts. Theor Ecol 3:163–174

Depuydt PO, Lambrecht BN, Joos GF, Pauwels RA (2002) Effect of ozone exposure on allergic sensitization and airway inflammation induced by dendritic cells. Clin Exp Allergy 32:391–396

Drake JM, Griffen BD (2010) Early warning signals of extinction in deteriorating environments. Nature 467:456–459

Fakhrzadeh L, Laskin JD, Laskin DL (2002) Deficiency in inducible nitric oxide synthase protects mice from ozone-induced lung inflammation and tissue injury. Am J Respir Cell Mol Biol 26:413–419

Freijer JI, van Eijkeren JCH, van Bree L (2002) A model for the effect on health of repeated exposure to ozone. Environ Modell Softw 17:553–562

Frey U, Brodbeck T, Majumdar A, Taylor DR, Town GI, Silverman M, Suki B (2005) Risk of severe asthma episodes predicted from fluctuation analysis of airway function. Nature 438:667–670

Gerrity TR, McDonnell WF (1989) Do functional changes in humans correlate with the airway removal efficiency of ozone? In: Schneider T, Lee SD, Wolters GJR, Grant LD (eds) Atmospheric ozone research and its policy implications. Elsevier, Amsterdam, pp 293–300

Goutelle S, Maurin M, Rougier F, Barbaut X, Bourguignon L, Duncher M, Maire P (2008) The Hill equation: a review of its capabilities in pharmacological modeling. Fund Clin Pharmacol 22:633–648

Guttal V, Jayaprakash C (2008) Changing skewness: an early warning signal of regime shifts in ecosystems. Ecol Lett 11:450–460

Hill AV (1910) The possible effects of the aggregation of the hemoglobin on its dissociation curves. J Physiol 40:4–7

Hsieh NH, Liao CM (2013) Fluctuations in air pollution give risk warning signals of asthma hospitalization. Atmos Environ 75:206–216

Inoue H, Aizawa H, Nakano H, Matsumoto K, Kuwano K, Nadel JA, Hara N (2000) Nitric oxide synthase inhibitors attenuate ozone-induced airway inflammation in guinea pigs: possible role of interleukin-8. Am J Resp Crit Care Med 161:249–256

Jakab GJ, Spannhake EW, Canning BJ, Kleeberger SR, Gilmour MI (1995) The effects of ozone on immune response. Environment Health Perspect 103:77–89

Jerrett M, Burnett RT, Pope CA, Ito K, Thurston G, Krewski D, Shi YL, Calle E, Thun M (2009) Long-term ozone exposure and mortality. N Engl J Med 360:1085–1095

Kim SE, Kumar A (2005) Accounting seasonal nonstationarity in time series models for short-term ozone level forecast. Stoch Environ Res Risk Assess 19:241–248

Kleeberger SR, Ohtsuka Y, Zhang LY, Longphre M (2001) Airway responses to chronic ozone exposure are partially mediated through mast cells. J Appl Physiol 90:713–723

McConnell R, Berhane K, Gilliland F, London SJ, Islam T, Gauderman WJ, Avol E, Margolis HG, Peters JM (2002) Asthma in exercising children exposed to ozone: a cohort study. Lancet 359:386–391

McDonnell WF, Stewart PW, Smith MV (2010) Prediction of ozone-induced lung function responses in humans. Inhal Toxicol 22:160–168

Moral FJ, Rebollo FJ, Méndez F (2014) Using an objective model to estimate overall ozone levels at different urban locations. Stoch Environ Res Risk Assess 28:455–465

Mudway IS, Kelly FJ (2000) Ozone and the lung: a sensitive issue. Mol Aspects Med 21:1–48

National Research Council (2008) Estimating mortality risk reduction and economic benefits from controlling ozone air pollution. National Academy Press, Washington 2008

Neuhaus-Steinmetz U, Uffhausen F, Herz U, Renz H (2000) Priming of allergic immune responses by repeated ozone exposure in mice. Am J Respir Cell Mol Biol 23:228–233

Park SK, O'Neill MS, Vokonas PS, Sparrow D, Schwartz J (2005) Effects of air pollution on heart rate variability: the VA normative aging study. Environ Health Perspect 113:304–309

Scheffer M, Bascompte J, Brock WA, Brovkin V, Carpenter SR, Dakos V, Held H, van Nes EH, Rietkerk M, Sugihara G (2009) Early-warning signals for critical transitions. Nature 461:53–59

Schelegle ES, Morales CA, Walby WF, Marion S, Allen RP (2009) 6.6-Hour inhalation of ozone concentrations from 60 to 87 parts per billion in healthy humans. Am J Resp Crit Care Med 180:265–272

Tank J, Biller H, Heusser K, Holz O, Diedrich A, Framke T, Koch A, Grosshennig A, Koch W, Krug N, Jordan J, Hohlfeld JM (2011) Effect of acute ozone induced airway inflammation on human sympathetic nerve traffic: a randomized, placebo controlled, crossover study. PLoS ONE 6:e18737

Venegas JG, Winkler T, Musch G, Melo MFV, Layfield D, Thavalekos N, Fischman AJ, Callahan RJ, Bellani G, Harris RS (2005) Self-organized patchiness in asthma as a prelude to catastrophic shifts. Nature 434:777–782

Weinhold B (2008) Ozone nation: ePA standard panned by the people. Environ Health Perspect 116:A302–A305

World Health Organization (2006) Air quality guidelines for particulate matter, ozone, nitrogen dioxide and sulfur dioxide. World Health Organization Press, Washington 2006